Cancer & Metabolism

RESEARCH Open Access

RNF2 promotes chondrosarcoma progression by regulating ubiquitination and degradation of CBX7

Yue Wu[1†], Zheng Huang[2†], Ping Luo[3*], Zhong Xiang[3], Meng Zhang[3], Zhiwu Chen[3], Yalu Zhou[3] and Jiameng Li[3]

Abstract

Objective Chondrosarcoma (CHS) is resistant to conventional chemotherapy and radiotherapy and currently lacks effective treatment options when in advanced stages. Accordingly, this research investigated the mechanism of RNF2/CBX7 in CHS to drive the development of molecularly targeted drugs for CHS.

Methods RNF2 and CBX7 levels were detected in CHS cells and tissues. RNF2 and CBX7 expression was modulated through cell transfection to examine their effects on cell proliferation, apoptosis, migration, and angiogenesis. The correlation between RNF2 and CBX7 levels was determined, and the ubiquitination level of CBX7 was tested. Protein synthesis was blocked in RNF2-knockdown/overexpressing cells with CHX to assess the effect of RNF2 on CBX7 stability. JJ012 cells transfected with LV-sh-RNF2 were subcutaneously injected into nu/nu nude mice to ascertain the action of RNF2 in the growth and metastasis of CHS.

Results RNF2 was highly expressed in CHS cells and tissues. RNF2 knockdown curbed CHS cell proliferation, migration, and angiogenesis while promoting apoptosis. RNF2 knockdown in JJ012 cells upregulated CBX7 protein levels and reduced CBX7 ubiquitination, whilst RNF2 had no effect on CBX7 mRNA expression. CBX7 knockdown partially nullified the repressing effects of RNF2 knockdown on CHS cell proliferation, migration, and angiogenesis, and CBX7 overexpression partially abolished the promotional effects of RNF2 overexpression. LV-sh-RNF2 prominently restricted tumor growth and weight and declined lung metastatic nodules and Ki-67-positive cells in mice.

Conclusion RNF2 fosters CHS progression by elevating CBX7 degradation via the ubiquitination pathway.

Keywords Chondrosarcoma, RNF2, CBX7, Ubiquitination, Metastasis

†Yue Wu and Zheng Huang contributed equally to this work.

*Correspondence:
Ping Luo
luopingspine@126.com
[1]Department of Orthopedics, Beijing Chaoyang Hospital, No.8 Gongti South Rd, Chaoyang District, Beijing 100020, China
[2]Department of Orthopedics, Huazhong University of Science and Technology Union Shenzhen Hospital, No. 89 Taoyuan Road, Nanshan District, Shenzhen City 210009, Guangdong, China
[3]Department of Spinal Surgery, The Fourth Hospital of Changsha, Changsha Hospital of Hunan Normal University, No.70 Lushan Road, Yuelu District, Changsha 410006, Hunan, China

Introduction

Chondrosarcoma (CHS) is a malignant tumor composed of hyaline cartilage matrix and chondrocytes, which is the second most prevailing primary solid bone tumor next to osteogenic sarcoma, accounting for 20−27% of all primary malignant bone tumors [1–3] and mainly affecting adults. The 5-year survival rates for patients with low-grade, high-grade, and dedifferentiated CHS have been reported as 83%, 53%, and 7−24%, respectively [4, 5]. Most CHS cases are slow-growing and rarely metastatic, with a favorable prognosis in the presence of adequate surgical treatment. However, high-grade CHS requires extensive surgical resection due to high resistance to chemotherapy and radiotherapy [6–8]. Therefore, treatment regimens for patients with metastatic or unresectable CHS are limited, and new therapeutic methods, such as molecularly targeted agents and immunotherapy, are required [4]. However, the pathogenesis of CHS has not been fully elucidated, hinting at an urgent need to explore the molecular mechanisms of CHS pathogenesis and develop novel therapeutic strategies.

Ubiquitination, as a key post-translational modification in normal homeostasis and diseases, involves the covalent attachment of ubiquitin to target proteins for proteasomal degradation or non-degradation signaling [9], which marks proteins for degradation via proteasomes, alters cellular location, affects their activity, and promotes or prevents protein interactions [10]. In cancers, ubiquitination regulates tumor-inhibiting and tumor-promoting pathways in an environment-dependent manner [11–14]. A few studies have reported the involvement of ubiquitination in CHS. For instance, the protein-based ubiquitination inhibitor MLN4924 inhibits the growth of human CHS by reducing cell proliferation and inducing apoptosis [15]. The E3 ubiquitin ligase FBXW11 in CHS tissues is lower than that in normal tissues and benign cartilage tumor tissues [16]. RNF2 (ding, Ring1B, or Ring2), belonging to the Ring finger protein family, is an E3 ubiquitin ligase implicated in the mono-ubiquitination of histone H2A at lysine 119 (H2AK119ub). RNF2 overexpression is involved in the pathological progression of a wide range of tumors and has an impact on their clinical features [17, 18]. However, the effect of RNF2 on CHS is still unknown.

Polycomb-group proteins are crucial for the epigenetic regulation of transcription and play an important role in chromatin remodeling. The Chromobox (CBX) gene family is an essential component of the canonical polycomb repressor complex 1, which participates in chromatin remodeling. CBX mediates epigenetic gene silencing and is implicated in cancer development [19, 20]. Although CBX7 has been unveiled to repress the progression of bladder [21] and breast cancers [22], its role in CHS has not yet been reported. In the present study, the website UbiBrowser (http://ubibrowser.bio-it.cn/ubibrowser_v3/) predicted that CBX7 was a downstream ubiquitination substrate for RNF2. Based on the above findings, we hypothesized that RNF2 may promote CHS progression by degrading CBX7 through the ubiquitination pathway. Accordingly, this study probed the role and regulatory mechanism of the RNF2/CBX7 axis in CHS through clinical, cellular, and animal experiments, providing data references for the potential application of RNF2/CBX7 in molecularly targeted drugs for CHS.

Methods

Sample collection

Tissue specimens were obtained from 25 CHS patients who underwent surgery in the Fourth Hospital of Changsha, Changsha Hospital of Hunan Normal University from January 2019 to December 2021. The following inclusion criterion were used: cases were diagnosed by both imaging and pathology. Exclusion criteria were as follows: age<18 years or >70 years; combination with neurological lesions such as cerebral hemorrhage or cerebral infarction; combination with systemic metabolic diseases such as diabetes; combination with other malignant tumors; and combination with Hepatitis B virus and human immunodeficiency virus. Normal cartilage tissues from 25 patients with amputations due to car accidents or other accidental injuries were selected as the control. The patients were informed and signed an informed consent before specimen collection, and the study protocol and procedures were ratified by the Ethics Committee of the Fourth Hospital of Changsha, Changsha Hospital of Hunan Normal University (Approval number: 2023LL0901001).

Cell culture

Normal human chondrocytes C-28/I2 and CHS cell lines JJ012, SW1353, OUMS-27, and HCS-2/8 (ATCC, USA) were used. C-28/I2 and JJ012 cells were maintained in a Roswell Park Memorial Institute-1640 medium (Invitrogen, Carlsbad, CA, USA) encompassing 10% FBS and 1% penicillin/streptomycin at 37℃ under humidified conditions with 5% CO_2. SW1353 cells were maintained in a L-15 medium, while OUMS-27 and HCS-2/8 cells were cultured in a Dulbecco's Modified Eagle Medium encompassing 10% FBS and 1% penicillin/streptomycin.

Reverse transcription-quantitative polymerase chain reaction (RT-qPCR)

RNA was extracted from tissue specimens or cells using TRIzol reagents (azyme, Nanjing, China), with the purity and concentration of RNA determined on the NanoDrop 2000 spectrophotometer (Thermo Fisher Scientific, USA). cDNA was synthesized with the FastQuant RT kit (with gDNase; TianGen, Beijing, China). Next, RT-qPCR

Table 1 Primer sequence in RT-qPCR

Gene	Forward 5′-3′	Reverse 5′-3′
RNF2	GTGTGTGGATGTGTGTTT	ATGTGGCTATGTATATGTTACC
CBX7	GGATGGCCCCCAAAGTACAG	TATACCCCGATGCTCGGTCTC
GAPDH	AATCCCATCACCATCTTCCAG	AAATGAGCCCCAGCCTTC

Table 2 Sequences of shRNAs used in this study

Definition	sequences
sh-RNF2	5′-UAUCACUUUCUGUUUCAGCUG-3′
sh-CBX7	5′-CAAAGTACAGCACGTGGGA-3′
sh-NC	5′-GTTCTCCGAACGTGTCACGT-3′

was carried out on the ABI7500 system using SYBR Premix Ex TaqII (Takara). With GAPDH as the internal reference, data were analyzed using the $2^{-\Delta\Delta Ct}$ method [23]. The primers (Table 1) were synthesized by Sangon (Shanghai, China).

Western blot

Total proteins were extracted from clinical tissue specimens or cells with Radioimmunoprecipitation Assay lysis buffer encompassing protease inhibitor (Beyotime, Shanghai, China), and then the protein concentration was measured with bicinchoninic acid kits (Beyotime). Equal amounts of proteins were subjected to sodium dodecyl-sulfate polyacrylamide gel electrophoresis and transferred onto polyvinylidene fluoride membranes, which were blocked with 5% non-fat milk in Tris Buffered Saline Buffer with Tween 20 for 1 h before overnight incubation with primary antibodies [Abcam; 1:1000; RNF2 (ab181140), CBX7 (ab21873), and β-tubulin (the control, ab179511)] at 4 °C and 1 h of incubation with immunoglobulin G (IgG) H&L (horseradish peroxidase [HRP]) secondary antibodies (GAR007, Multi science, Hangzhou, China). Protein bands were visualized with an Amersham ECL detection kit. ImageJ software (RRID: SCR_003070) was applied for protein quantification.

Immunohistochemistry (IHC)

RNF2 levels in tissues were assessed by IHC staining [24]. Paraffin sections of CHS tissues and normal cartilage tissues were dewaxed and rehydrated, followed by treatment with Target Retrieval Solution and 0.3% hydrogen peroxide. Subsequent to overnight incubation with anti-RNF2 (1:100; ab187509, Abcam) at 4 °C and 30-min incubation with HRP-IgG (Maxim-Bio, Fuzhou, China), the sections were subjected to diaminobenzidine treatment, hematoxylin staining, and final observation under an optical microscope (x200; Olympus, Japan).

Cell transfection

The synthesized short hairpin RNA (sh)-RNF2, sh-CBX7, and sh-negative control (NC) were inserted into pGPU6-GFP-Neo shRNA vectors to construct shRNAs targeting RNF2 and CBX7 and controls. The coding region of RNF2/CBX7 was inserted into pcDNA3.1(+)/Myc-His A vectors (Invitrogen) to obtain RNF2/CBX7 overexpression vectors. CHS cells (5×10^5 cells/well) were cultured to 50% confluence in 6-well plates one day before transfection and then transfected with different transfectants (100 nM) using Lipofectamine 2000 (Invitrogen). Cells were attained 48 h following transfection and screened by puromycin for stable clones. All shRNAs and plasmids used were designed by GenePharma (Shanghai, China). Sequences for the shRNAs are exhibited in Table 2.

Cell counting kit (CCK)-8 assay

JJ012/SW1353 cells were cultured for 0/24/48/72 h and subjected to 4-h incubation with 10 μL of enhanced CCK-8 solutions (C0042, Beyotime) at 37 °C. Cell viability was determined at 450 nm using a microplate reader (Thermo).

5-ethynyl-2′-deoxyuridine (EdU) assay

Cells were cultured for 48 h and incorporated with 20 μM EdU solutions (C10310-1, RiboBio, Guangzhou, China) for 2 h. After being fixed and permeabilized, cells were stained with EdU solutions for 30 min and treated with 4′,6-Diamidino-2-Phenylindole for 30 min. Finally, the images were captured using an IX71 microscope (Olympus). EdU-positive cells were counted from 10 random areas, with a minimal number of more than 500 cells.

Flow cytometry

JJ012/SW1353 cells were cultured in ultra-low attachment 6-well plates for 3 days prior to detection. Then, 1×10^6 cells were detected using an Annexin V-FITC/PI kit (BD Biosciences, USA). Apoptotic cells were analyzed by a flow cytometer (BD Biosciences).

Scratch assay

JJ012/SW1353 cells in 6-well plates were cultured in a complete medium (CM) upon 90% confluence. Next, a pipette tip (10 μL) was utilized to create wounds. Cell migration to the wound at 0 and 24 h was monitored

with an inverted light microscope and quantified by measuring the distance.

Tube formation assay

CM was used to culture JJ012 and SW1353 cells. Cells were washed thrice with PBS, transferred to a serum-free medium, and cultured upon 70−80% confluence. Then, CM was obtained 24 h following medium replacement and preserved at -80℃ until use.

Matrigel (BD Biosciences) was dissolved overnight at 4°C. A pre-chilled 96-well plate coated with thawed Matrigel (50 μL) was incubated for 30 min at 37 °C. After Matrigel was solidified, 1×10^4 human umbilical vein endothelial cells (HUVECs; ATCC) were suspended in the medium containing 50% CM and seeded in the wells. After 4–12 h, tube formation at 6 h was photographed, and tube branches and total tube length were determined with ImageJ software. Their number represented the capacity of angiogenesis.

Coimmunoprecipitation assay (Co-IP) assay

The Co-IP assay was conducted to assess the interaction between RNF2 and CBX7. Total proteins were extracted subsequent to 24 h of cell culture. Part of quantified total proteins was set as input. Equivalent proteins were probed with anti-RNF2 (Proteintech) or anti-CBX7 (Proteintech) at 4 °C overnight and then with Protein A/G at 4 °C for 6 h. Immunoprecipitates were attained as the Co-IP group. At last, the proteins were detected by Western blot using anti-RNF2 or anti-CBX7 antibodies.

Cycloheximide (CHX) chase and in vivo CBX7 ubiquitination assay

To test CBX7 protein stability, sh-RNF2 and pcDNA3.1-RNF2 were separately transfected into JJ012 and SW1353 cells for 36 h. Next, cells were treated with CHX (50 μg/mL; Sigma) and collected at the indicated time points, and cell lysates were utilized for Western blot.

For the ubiquitination of CBX7, JJ012/SW1353 cells were co-transfected with pcDNA3.1-CBX7 and pcDNA3.1-RNF2/sh-RNF2 or hemagglutinin-tagged ubiquitin (HA-Ub). After 36 h, cells were added with MG132 (30 μM) for 4 h. Next, the proteins were extracted and boiled for 10 min prior to cellular debris removal by centrifugation. Subsequently, the cell lysate was diluted 10 times with NP-40 lysis buffer, and immunoprecipitation was conducted with anti-Myc-Tag. Following overnight incubation, protein A/G-agarose (Santa Cruz) complexes were added, and the lysate was rotated for 2–4 h before three washes with NP-40 lysis buffer. Finally, Co-IP and input proteins were detected by Western blot using anti-CBX7 or anti-ubiquitin (1:1000, Proteintech) antibodies. Related plasmids including Myc-CBX7, Flag-RNF2, and HA-Ub were purchased from GeneChem (Shanghai, China). Transfection was performed using Lipofectamine 2000 (Invitrogen).

Mouse modeling

Finally, the impact of RNF2 on tumor growth in vivo was verified through a transplant tumor model. To eliminate the sex difference between groups and ensure the balance between groups, nu/nu female mice (specific pathogen-free grade; 6−8 weeks old; Vital River, Beijing, China) was selected for the present research. The synthetic pHBLV-U6-MCS-CMV-ZsGreen-PGKPuro lentiviral vector containing sh-RNF2 (LV-sh-RNF2), as well as LV-sh-NC, was constructed by GenePharma. A nude mouse transplant tumor model was developed [25]. JJ012 cells (100 μL; 1×10^6 cells) delivered with LV-sh-RNF2 or LV-sh-NC were mixed with 300 μL of Matrigel™ (BD Biosciences) and injected subcutaneously into the back of female nude mice. Tumor and lung tissues were acquired after 4 weeks.

Tumor size was metered throughout the experiment and tumor weight was measured at excision. Tumor volume (cm^3) was calculated as $ab^2/2$ [a: long diameter (cm); b: short diameter]. Part of the tumor was fixed overnight in 10% formalin and paraffin-embedded for hematoxylin and eosin (HE) staining. Part of the tumor was stored in RNAlater for RNA extraction or in lysis buffer for protein extraction. A mouse model of lung metastasis was constructed by the tail vein injection of JJ012 cells (2×10^6) stably expressing sh-RNF2. Metastatic burden was quantified as the number of nodules per lung [26]. All animal experiments were approved by the Animal Care and Use Committee and were conducted in strict compliance with the National Institutes of Health Guide for the Care and Use of Laboratory Animals. Animal suffering was minimized during experimental procedures.

Statistical analysis

GraphPad Prism 8.01 software was employed for statistical analysis and graphing of data. Data were verified to be normally distributed in the Shapiro-Wilk test and displayed as mean±standard deviation. Comparisons between two groups were performed using the independent samples *t*-test, and comparisons among multiple groups were analyzed by one-way analysis of variance, with Tukey's test for post hoc analysis. $P<0.05$ was considered statistically significant.

Results

RNF2 is highly expressed in CHS tissues and cells

To illustrate the role of RNF2 in CHS, we collected tissue specimens from CHS patients and normal cartilage tissue specimens from patients with amputations due to accidental injuries, such as car accidents, to examine RNF2 expression in clinical samples. RT-qPCR (Fig. 1A),

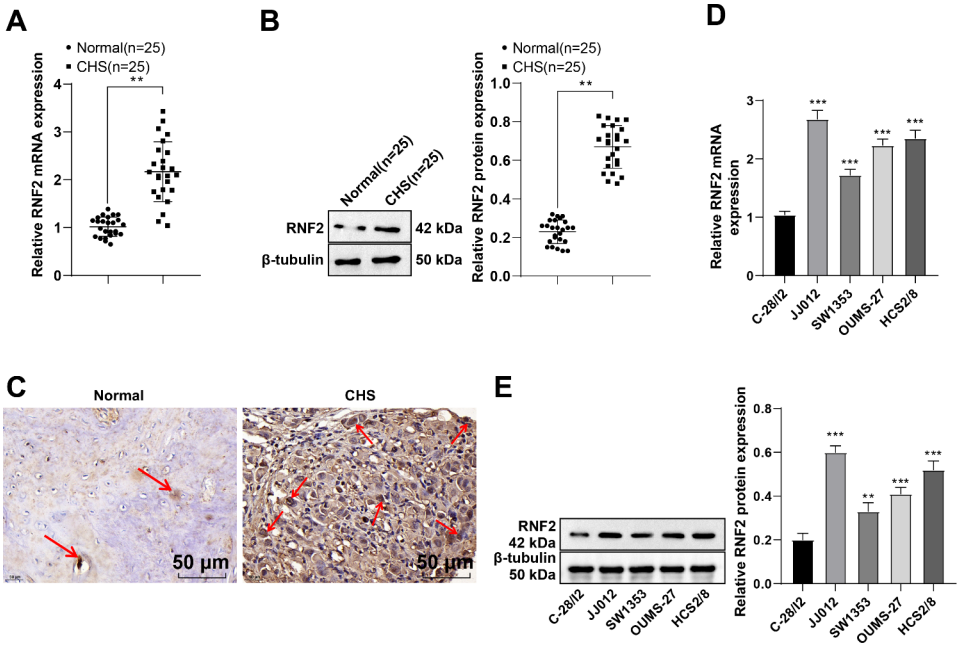

Fig. 1 High expression of RNF2 in CHS tissues and cells. Note: (**A**) RT-qPCR, (**B**) Western blot, and (**C**) immunohistochemistry (arrows indicate RNF2-positive cells) to detect RNF2 expression in CHS clinical samples ($N=25$); **, $P<0.01$ compared with the normal group; (**D**) RT-qPCR and (**F**) Western blot to detect RNF2 expression in CHS cell line. The cellular experiments were repeated three times, and the data were expressed as mean ± standard deviation. The independent samples *t*-test was used for comparisons between two groups, and one-way ANOVA was used for comparisons among multiple groups, with Tukey's multiple comparisons test for post hoc analysis. **, $P<0.01$, ***, $P<0.001$ compared with the C-28/I2 group

Western blot (Fig. 1B), and IHC (Fig. 1C) all showed substantially higher RNF2 expression in CHS patients than in normal controls (all $P<0.01$). Meanwhile, RT-qPCR (Fig. 1D) and Western blot (Fig. 1E) exhibited that compared with the normal chondrocyte C-28/I2 cells, RNF2 expression was higher in CHS cell lines (JJ012>HCS-2/8>OUMS-27>SW1353) (all $P<0.01$). In summary, RNF2 is upregulated in CHS and may be involved in CHS development.

RNF2 knockdown depresses CHS cell proliferation, migration, and angiogenesis while promoting apoptosis

To further ascertain the regulatory role of RNF2 in CHS, we knocked down RNF2 was knocked down in JJ012 cells via cellular transfection. RNF2 mRNA (Fig. 2A) and protein (both $P<0.01$, Fig. 2B) were prominently decreased in the sh-RNF2 group, indicating the successful transfection. CCK-8 (Fig. 2C) and EdU (Fig. 2D) assays demonstrated that RNF2 knockdown diminished JJ012 cell proliferation ($P<0.01$). Flow cytometry revealed that RNF2 knockdown increased JJ012 cell apoptosis ($P<0.01$, Fig. 2E). According to would healing assay results, RNF2 knockdown markedly lowered JJ012 cell migration ($P<0.01$, Fig. 2F). Tumor metastasis requires angiogenesis, which is a key factor in tumor progression [27, 28]. HUVECs were cultured using the CM of JJ012 cells in different groups. The tube formation assay displayed that the CM of RNF2-knockdown JJ012 cells evidently curbed tube formation of HUVECs ($P<0.01$, Fig. 2G). Altogether, RNF2 knockdown suppress CHS cell proliferation, migration, and angiogenesis and fosters apoptosis.

RNF2 overexpression promotes CHS cell proliferation, migration, and angiogenesis and limits apoptosis

Then, RNF2 was overexpressed in SW1353 cells with relatively low RNF2 expression through cellular transfection with pcDNA3.1-RNF2. RNF2 mRNA (Fig. 3A) and protein levels (both $P<0.01$, Fig. 3B) in the pc-RNF2 group were greatly higher than those in the pc-NC group, indicating the successful transfection. RNF2 overexpression accelerated cell proliferation (Fig. 3C/D), declined apoptosis (Fig. 3E), and augmented cell migration (Fig. 3F) and angiogenesis (all $P<0.01$, Fig. 3G). In short, RNF2 overexpression drives CHS cell proliferation, migration, and angiogenesis while limiting apoptosis.

RNF2 reduces CBX7 expression in CHS cells

CBX7 has been reported to impede the progression of many tumors [21, 22], but its role in CHS has not yet been reported. The website UbiBrowser (http://ubibrowser.bio-it.cn/ubibrowser_v3/) predicted that CBX7 was a downstream ubiquitination substrate for RNF2 (Fig. 4A). We hypothesized that RNF2 may facilitate CHS progression by degrading CBX7 *via* the ubiquitination pathway. Western blot exhibited that CBX7 expression in CHS tissues was markedly lower than that in normal

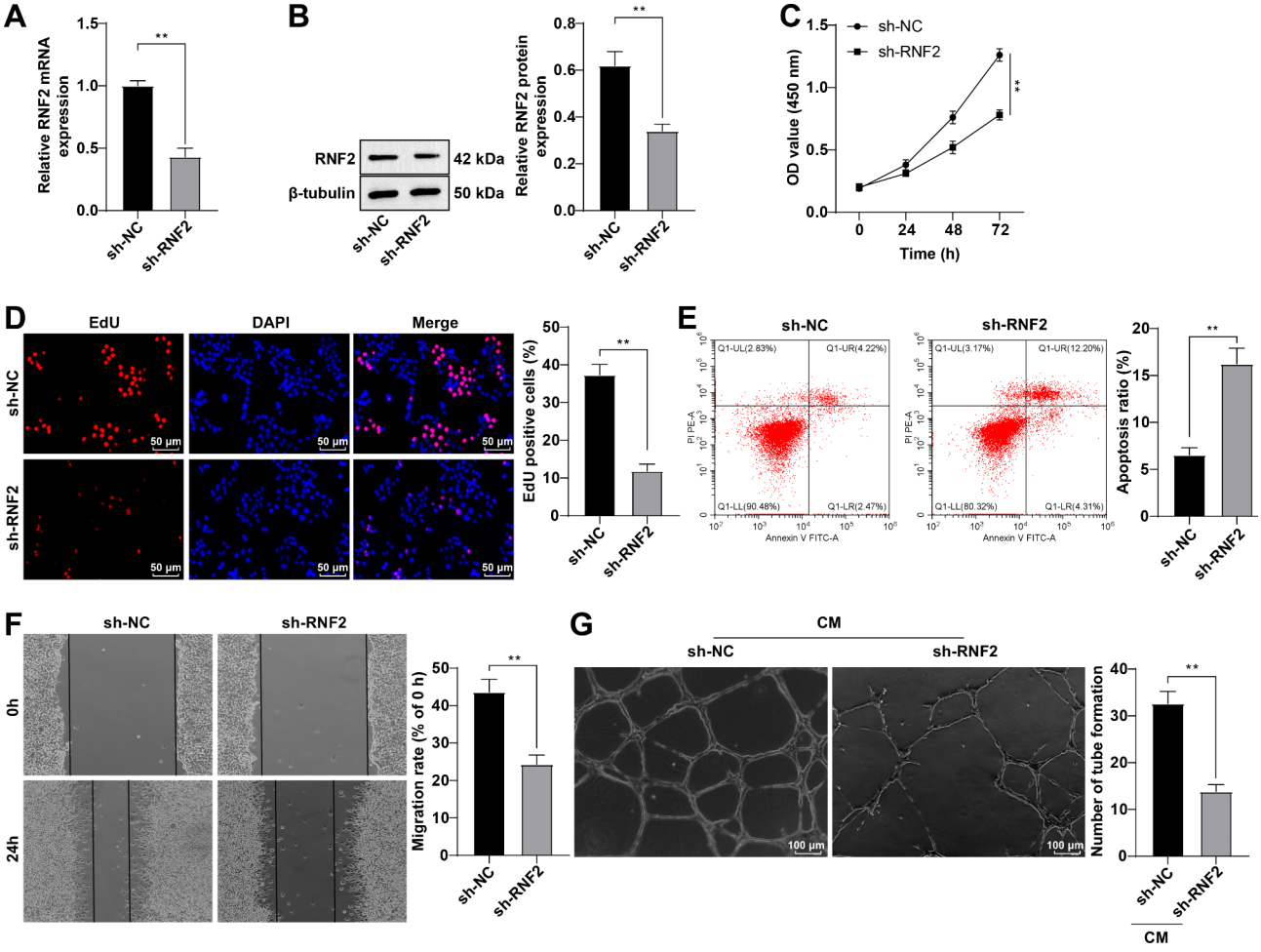

Fig. 2 RNF2 knockdown inhibits proliferation, migration, and angiogenesis and promotes apoptosis in JJ012 cells. Note: sh-RNF2 and sh-NC were transfected into JJ012 cells, respectively. (**A**) RT-qPCR and (**B**) Western blot to detect RNF2 mRNA and protein expression in JJ012 cells; (**C**) CCK-8 to detect JJ012 cell viability; (**D**) EdU to detect JJ012 cell proliferation; (**E**) FITC/PI staining to calculate the number of early and late cell deaths for detecting JJ012 cell apoptosis; (**F**) Scratch assay to observe the migration distance of cells on the plate at 0 h and 24 h, respectively, for assessing JJ012 cell migratory capabilities; (**G**) After culture of HUVECs with conditioned media of JJ012 cells in different groups, tube formation assay to observe the number of tubules for evaluating JJ012 cell angiogenic capabilities. The cellular experiments were repeated three times, and the data were expressed as mean ± standard deviation. The independent samples *t*-test was used for the comparison between two groups. ** $P < 0.01$

cartilage tissues ($P < 0.01$, Fig. 4B). RNF2 expression was negatively correlated with CBX7 expression in CHS tissues ($P < 0.01$, Fig. 4C). RNF2 knockdown in JJ012 cells resulted in upregulation of CBX7 protein levels, and RNF2 overexpression in SW1353 cells lowered CBX7 protein levels. Additionally, RNF2 had no effect on CBX7 mRNA expression (Fig. 4D-G). Further, the interaction between RNF2 and CBX7 in CHS was confirmed by the Co-IP assay (Fig. 4H/I). Above all, RNF2 inhibits CBX7 levels in CHS cells.

RNF2 promotes CBX7 ubiquitination in CHS cells

Considering the function of RNF2 family members to foster the degradation of their target proteins, we hypothesized that RNF2 may downregulate CBX7 protein by accelerating its degradation. Protein synthesis was blocked with CHX, followed by the measurement of CBX7 protein levels in RNF2-overexpressing/knockdown cells. The results revealed that CBX7 degradation was strikingly reduced and its half-life was prolonged in RNF2-knockdown JJ012 cells (Fig. 5A). Conversely, CBX7 half-life was shortened and its degradation was increased in RNF2-overexpressing SW1353 cells (Fig. 5B). The study then probed the pathways involved in RNF2-mediated CBX7 degradation. RNF2-induced CBX7 degradation was reversed by the proteasome inhibitor MG132 but not by the lysosomal inhibitor chloroquine or the autophagy inhibitor 3-MA, illustrating that RNF2 mediated CBX7 degradation through the proteasomal pathway (Fig. 5C). Next, the study assessed whether the E3 ubiquitin ligase RNF2 could mediate CBX7 ubiquitination. After co-transfection of Myc-CBX7 and HA-Ub or

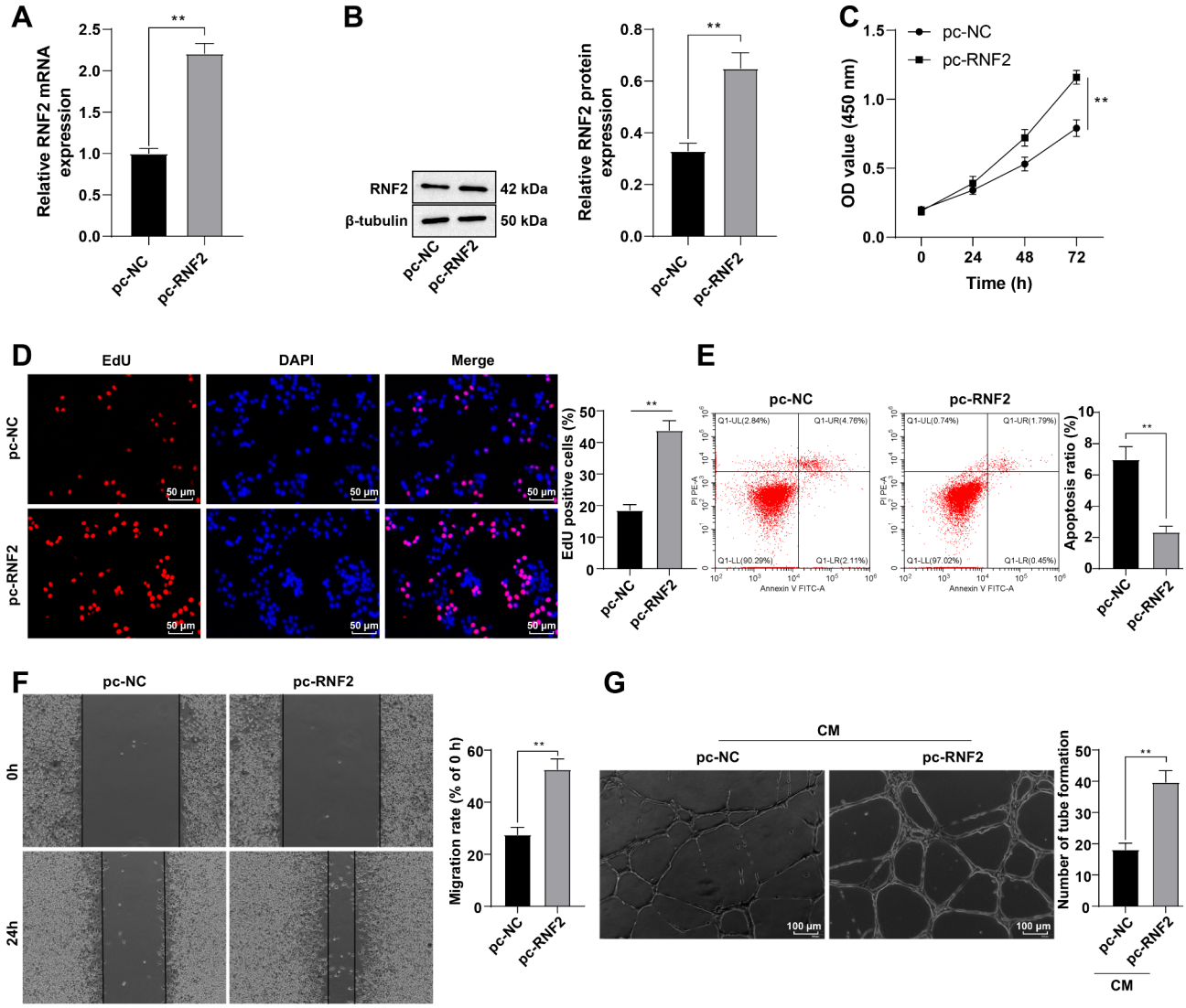

Fig. 3 Overexpression of RNF2 promotes proliferation, migration, and angiogenesis while inhibiting apoptosis in SW1353 cells. Note: pcDNA3.1-RNF2 and pcDNA3.1-NC were transfected into SW1353 cells, respectively. (**A**) RT-qPCR and (**B**) Western blot to detect RNF2 mRNA and protein expression in SW1353 cells; (**C**) CCK-8 to detect SW1353 cell viability; (**D**) EdU to detect SW1353 cell proliferation; (**E**) FITC/PI staining to calculate the number of early and late cell deaths for detecting SW1353 cell apoptosis; (**F**) Scratch assay to observe the migration distance of cells on the plate at 0 h and 24 h, respectively, for assessing SW1353 cell migratory capabilities; (**G**) After culture of HUVECs with conditioned media of SW1353 cells in different groups, tube formation assay to observe the number of tubules for evaluating SW1353 cell angiogenic capabilities. The cellular experiments were repeated three times, and the data were expressed as mean ± standard deviation. The independent sample *t*-test was used for the comparison between two groups. ** $P < 0.01$

Flag-RNF2, a significant increase in CBX7 ubiquitination was observed when RNF2 was present (Fig. 5D).

Consistent with the role of RNF2 directly involved in CBX7 ubiquitination, CBX7 ubiquitination was reduced when RNF2 was knocked down in JJ012 cells, whereas RNF2 overexpression enhanced exogenous CBX7 ubiquitination in cells (Fig. 5E).

Polyubiquitin chains are predominantly generated through two types of bonds, namely Lys48 and Lys63 chains. Through the use of specific ubiquitin mutants, it was identified that RNF2 effectively facilitated Lys48-linked CBX7 polyubiquitination but not Lys63-linked CBX7 polyubiquitination (Fig. 5F). Collectively, RNF2 promotes Lys48-linked CBX7 polyubiquitination in CHS cells.

RNF2 upregulation promotes CHS cell proliferation, migration, and angiogenesis and prevents apoptosis by lowering CBX7 expression

Rescue experiments were performed by knocking down both RNF2 and CBX7 in JJ012 cells ($P<0.01$, Fig. 6A) and by overexpressing both RNF2 and CBX7 in SW1353 cells ($P<0.01$, Fig. 6B). In JJ012 cells, CBX7 knockdown remarkably accelerated CHS cell migration, proliferation,

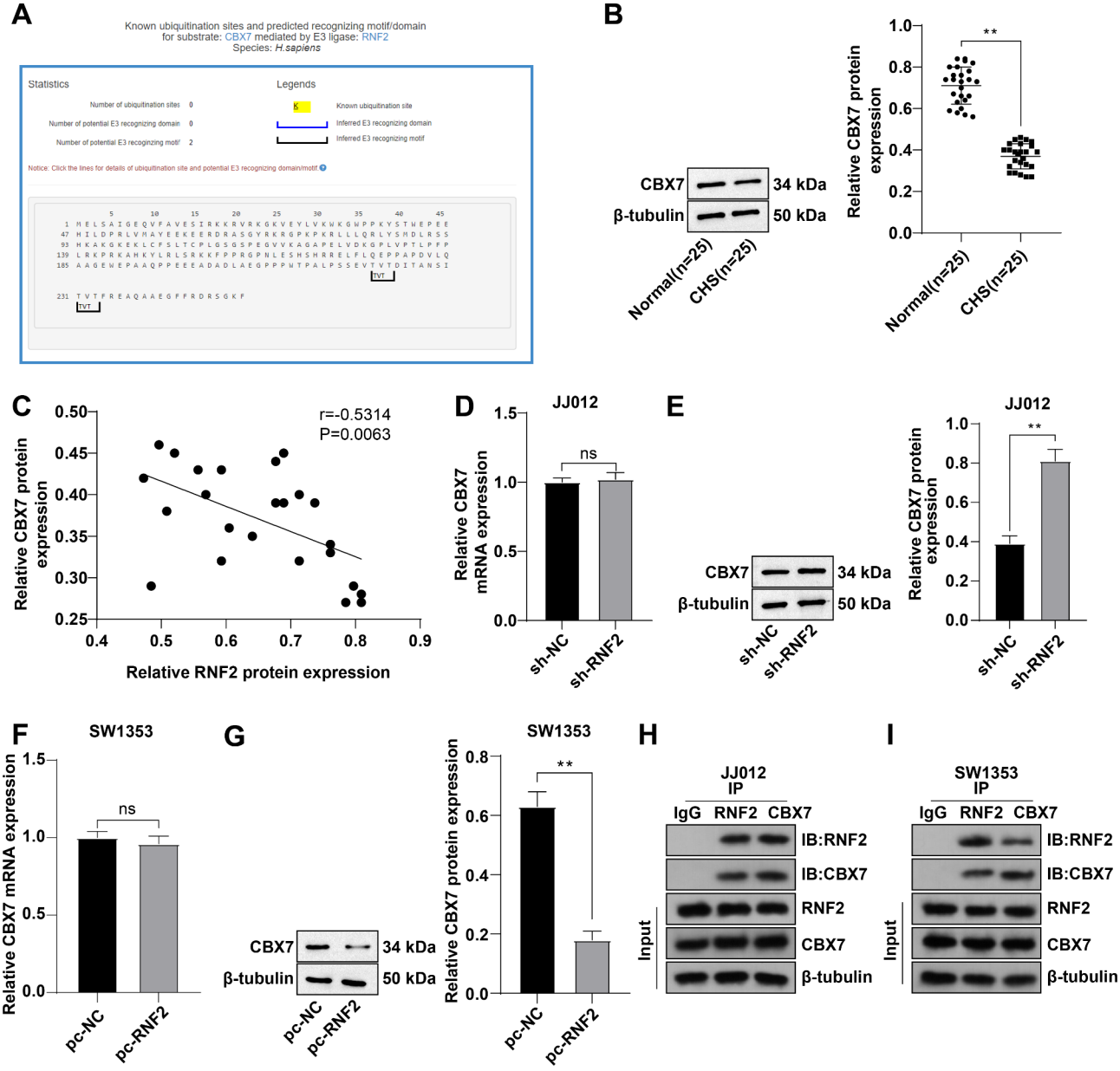

Fig. 4 RNF2 inhibits CBX7 expression in CHS cells. Note: (**A**) UbiBrowser website to predict the downstream ubiquitination substrate of RNF2; (**B**) Western blot to detect CBX7 levels in clinical samples; (**C**) Pearson method to analyze the correlation of RNF2 and CBX7 levels in CHS samples; (**D**/**F**) RT-qPCR and Western blot (E/G) to detect CBX7 mRNA and protein expression in JJ012 cells and SW1353 cells; (**H**/**I**) Co-IP to detect the interaction between RNF2 and CBX7 in CHS cells. The cellular experiments were repeated three times, and data were expressed as mean ± standard deviation. The independent samples *t*-test was used for comparisons between two groups. ** $P < 0.01$. ns, no statistical significance

and angiogenesis, and CBX7 knockdown partially reversed the inhibitory effects of RNF2 knockdown on CHS cells. Similarly, in SW1353 cells, overexpression of CBX7 decelerated cell proliferation, migration, and angiogenesis, partially nullifying the promotional effects of RNF2 overexpression ($P<0.01$, Fig. 6C-G). Altogether, RNF2 overexpression facilitates CHS cell migration, proliferation, and angiogenesis and hinders apoptosis by downregulating CBX7.

RNF2 overexpression promotes the growth and metastasis of CHS by repressing CBX7

Subsequently, JJ012 cells transfected with LV-sh-RNF2 or LV-sh-NC were subcutaneously injected into nu/nu nude mice on the back to establish a tumor-loading mouse model. Tumor growth and weight in the LV-sh-RNF2 group were dramatically reduced ($P<0.01$, Fig. 7A-C). HE staining showed that tumor cells in the LV-sh-NC group were of uneven size, with enlarged cell gaps, irregular arrangement, and increased inflammatory

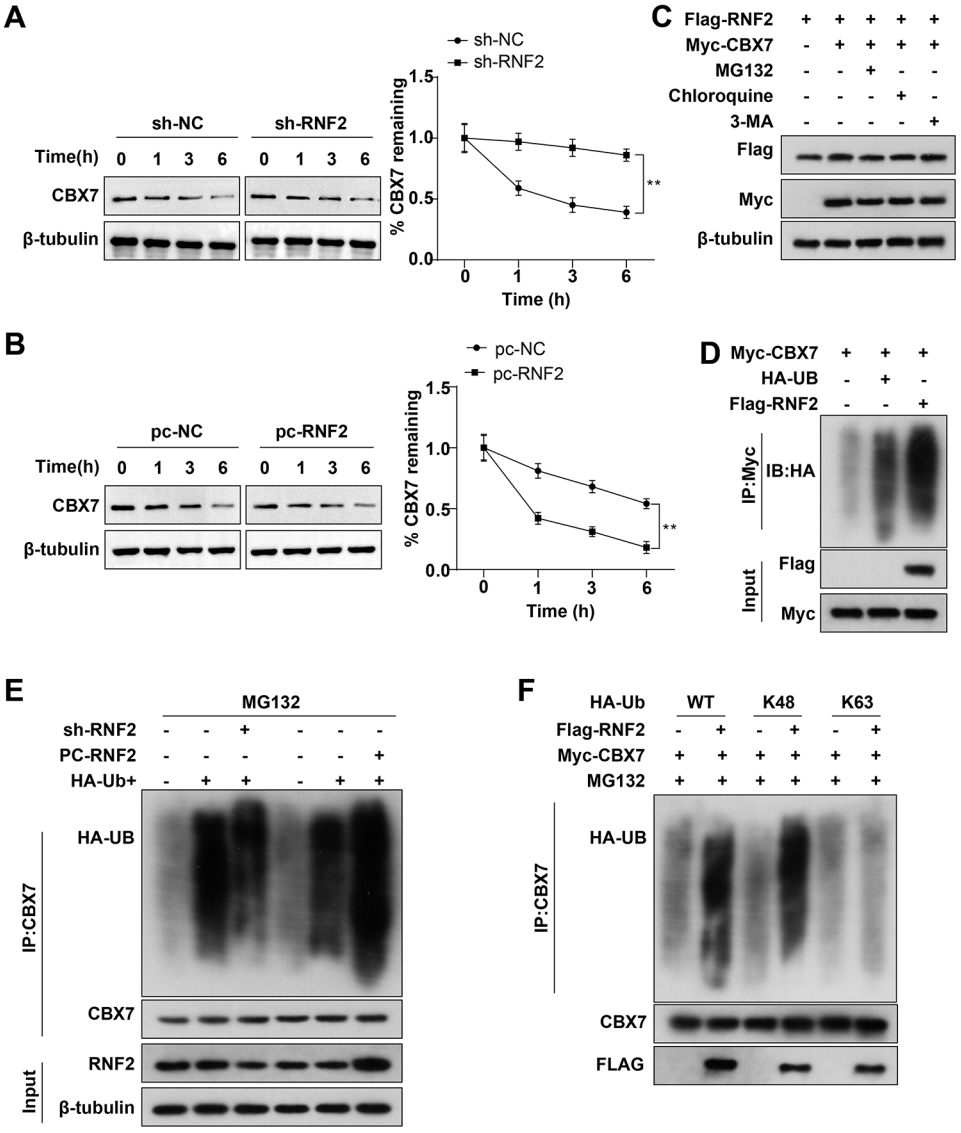

Fig. 5 RNF2 promotes ubiquitination of CBX7 in CHS cells. Note: (**A**/**B**) JJ012 cells/SW1353 cells after RNF2 knockdown or overexpression were treated with CHX, and CBX7 was detected by Western blot. The graph (lower panel) shows the percentage of remaining CBX7 protein level after CHX treatment; (**C**) JJ012 cells after RNF2 knockdown or overexpression were treated with MG132 (30 μM), chloroquine (10 mM), or 3-MA (10 mM) for 4 h. Cell lysates were prepared with SDS lysis buffer and used for Western blot; (**D**) Analysis of CBX7 ubiquitination after transfection of cells with plasmids expressing Myc-CBX7, Flag-RNF2, and HA-Ub; (**E**) JJ012 cells were co-transfected with the indicated RNAs and HA-Ub and treated with 30 μM MG132 for 4 h, followed by immunoblotting. (**F**) HEK-293T cells were co-transfected with Myc-CBX7 or Flag-RNF2 and the indicated HA-Ub WT, HA-K48-Ub (Lys48-only), or HA-K63-Ub (Lys63-only) plasmids, followed by immunoblotting analysis with anti-Flag antibodies to analyze the CBX7 ubiquitination. The cellular experiments were repeated three times and data were expressed as mean ± standard deviation. Comparisons between two groups were performed by the independent samples *t*-test. ** $P < 0.01$

cell infiltration, which indicated that tumor tissues were severely damaged. In contrast, tumor cells in the LV-sh-RNF2 group were tightly arranged, with a stable morphology and structure (Fig. 7D). In addition, lung metastatic nodules ($P<0.01$, Fig. 7E) and Ki-67-positive cells (Fig. 7F) were strikingly decreased in the LV-sh-RNF2 group. The LV-sh-RNF2 group had significantly lower RNF2 expression and remarkably higher CBX7 expression (both $P<0.01$, Fig. 7G). In all, RNF2 promotes CHS growth and metastasis by declining CBX7 expression.

Discussion

As the 2nd prevailing malignant bone tumor, CHS is primarily featured by cartilaginous matrix production [29]. CHS generally develops resistance to treatment modalities including chemotherapy and radiation, which makes it easily progress into unresectable or metastatic CHS, resulting in poor outcomes [4, 30]. Consequently, more

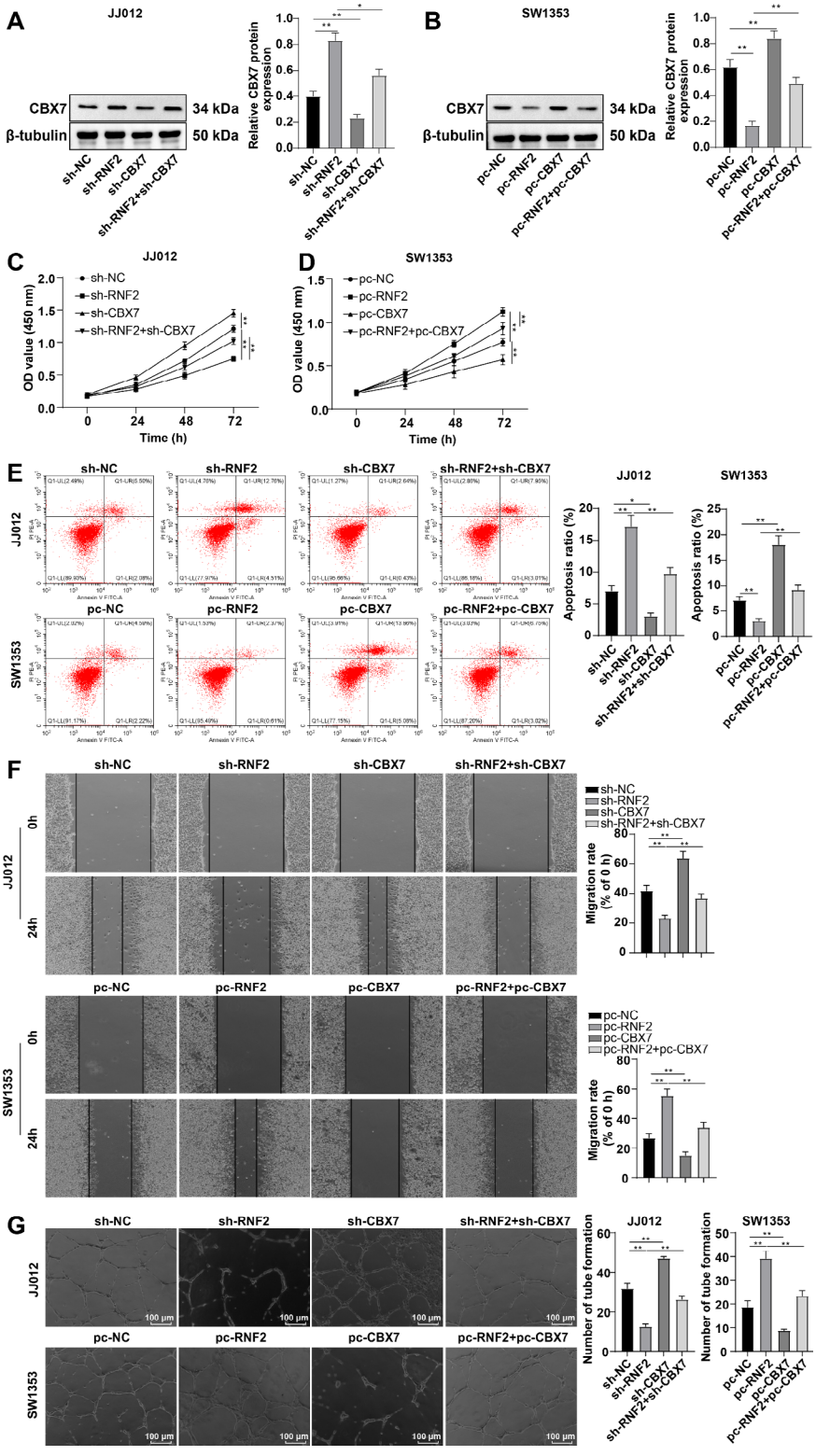

Fig. 6 RNF2 promotes CHS cell proliferation, migration, and angiogenesis and inhibits apoptosis by inhibiting CBX7 expression. Note: (**A**/**B**) Western blot to detect CBX7 protein expression; (**C**/**D**) CCK-8 to detect cell viability; (**E**) FITC/PI staining to calculate the number of early and late cell deaths for measuring apoptosis; (**F**) Scratch assay to observe the migration distance of cells on the plate at 0 h and 24 h, respectively, for determining cell migratory capabilities; (**G**) After culture of HUVECs with conditioned media of SW1353 cells in different groups, tube formation assay to observe the number of tubules for evaluating cell angiogenic capabilities. The cellular experiments were repeated three times, and data were expressed as mean ± standard deviation. One-way ANOVA was used for comparisons among multiple groups, and Tukey's multiple comparisons test was used for post-hoc analysis. * $P < 0.05$, ** $P < 0.01$

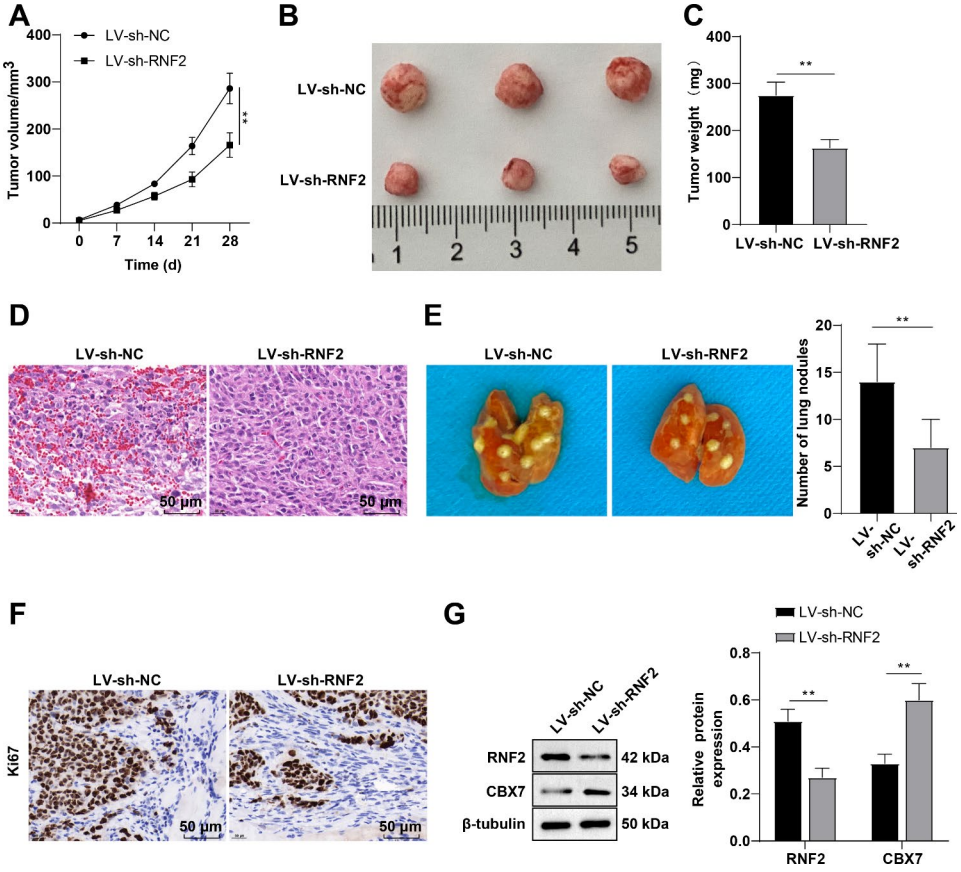

Fig. 7 RNF2 promotes CHS growth and metastasis by inhibiting CBX7. Note: JJ012 cells transfected with LV-sh-RNF2 or LV-sh-NC were dorsally injected subcutaneously into nu/nu nude mice to construct a hormonal mouse model. (**A**) Curve of changes in tumor volume over time; (**B**) Representative images of the tumors in each group; (**C**) Statistics of tumor weight in each group; (**D**) HE staining to observe the morphology of tumor tissues; (**E**) The number of lung nodules to assess tumor metastasis; (**F**) Positive expression of the proliferating factor Ki-67 tested with immunohistochemistry; (**G**) Western blot to detect the protein expression of RNF2/CBX7. Animal experiments: $n = 8$. Data were expressed as mean ± standard deviation, and the independent samples *t*-test was used for comparisons between two groups. ** $P < 0.01$ compared with the LV-sh-NC group

efforts are required to delve into the mechanisms behind CHS progression, thus developing promising therapeutic approaches. Recently, researchers have unearthed the extensive involvement of ubiquitination in tumor invasion and metastasis [14]. This study unveiled that RNF2, an E3 ubiquitin ligase, accelerated CBX7 degradation through ubiquitination, thereby facilitating the malignant progression of CHS.

Ubiquitination is considered a crucial post-translational modification involving the covalent attachment of ubiquitin to target proteins, resulting in proteasomal degradation or alternations in non-degradative signaling. In the ubiquitin system, components with cancer-related functions consist of E3 ligases, E1/2 enzymes, deubiquitinases, and proteasomes [12]. As an essential E3 ubiquitin ligase, RNF2 is not only implicated in the initiation and progression of multiple cancers but also exerts a vital impact on their clinical manifestations, showing potential clinical values in cancer diagnosis, therapy, and prognosis [17]. Importantly, RNF2 is upregulated in numerous human malignancies, and its overexpression is relevant to poor prognosis and short survival in cancer patients [31]. Consistently, our data indicated that RNF2 was highly expressed in CHS tissues and cells and that knockdown of RNF2 restrained cell proliferation, migration, and angiogenesis in CHS, as well as enhancing apoptosis, whereas overexpression of RNF2 encouraged the malignant behaviors of CHS cells. Although evidence about the role of RNF2 in CHS is scarce, several reports have demonstrated its role in other cancers. In Ewing sarcoma, RNF2 is critical for the expression patterns of key EWSR1-FLI1 targets by inducing oncogene recruitment to their enhancers, and its knockdown delays the growth of tumor xenografts [32]. RNF2 is implicated in the mechanism of BMI1 in accelerating proliferation and metastasis in osteosarcoma [33]. RNF2 knockdown not only effectively represses cell proliferation and anti-apoptosis via the regulation of MDM2 and p53 stability in colorectal cancer [34] but also weakens cell viability and cell cycle entry in gastric cancer [35]. Overall, our

findings underscored the facilitating impact of RNF2 on CHS cell growth.

E3 ubiquitin ligases are revealed to control eukaryotic biology by triggering protein ubiquitination and degradation [36]. It is well acknowledged that E3 ligases modulate ubiquitination substrates specifically within the ubiquitylation process [37]. Interestingly, online tools suggested CBX7 as a downstream ubiquitination substrate of RNF2. Mechanistically, RNF2 potentiated CBX7 ubiquitination to facilitate its degradation in CHS cells. As reported, CBX7 is lowly expressed in sarcoma (SARC), and its downregulation is related to short survival [38]. Compelling evidence has uncovered the action of CBX7 as a tumor suppressor in either humans or mice [39]. In the present study, CBX7 was weakly expressed in CHS tissues and negatively linked to RNF2. Next, the precise role of CBX7 in CHS development was explored. CBX7 silencing potentiated cell migration, proliferation, and angiogenesis and weakened apoptosis in CHS, which was contrary to the functions of CBX7 upregulation. It has been evidenced that CBX7 is negatively linked to malignant degree, clinical stage, vascular invasion, interstitial invasion, and lymphatic metastasis in cervical cancer [40] and that CBX7 overexpression also retards cancer cell motility and growth and stimulates apoptosis [41]. CBX7 is capable of counteracting the oncogenic action of HMGA proteins and inhibiting the expression of proliferation/migration-related genes, including CCNE and SPP1 [42]. Through modulation of AKR1B10/ERK signaling, ectopic expression of CBX7 can curb invasion, migration, proliferation, and stemness of urinary bladder cancer cells, whereas CBX7 depletion facilitates cancer cell aggressiveness [21]. CBX7 confers a tumor-suppressing role in both lung squamous cell carcinoma and adenocarcinoma by blocking the ERK/MAPK pathway [43]. Overexpression of CBX7 impairs cell self-renewal potentials in breast cancer partially via DKK-1-triggered repression of the Wnt/β-catenin pathway [22]. Subsequently, as displayed by rescue experiments, CBX7 silencing partly abrogated the repressing impact of RNF2 knockdown on the malignant behaviors of CHS cells, while CBX7 upregulation partly annulled the promoting role of RNF2 overexpression. In vivo assays further clarified the action of the RNF2/CBX7 axis in the development of CHS. Altogether, RNF2 upregulation boosted CHS progression by lowering CBX7 expression. Intriguingly, a prior study demonstrated that CBX4 loss could affect the expression of other CBX members [44]. Accordingly, additional studies are warranted to further explore whether RNF2 also influences the expression of other CBX members in addition to CBX7.

To sum up, this paper innovatively elucidated that RNF2 upregulation facilitated CBX7 degradation via ubiquitination, thus augmenting cell proliferation, migration, and angiogenesis and suppressing apoptosis in CHS. Our results provide novel insights into the mechanism of ubiquitination in CHS progression and promising targets for CHS management. However, clinical samples included in this research were limited, which calls for additional studies with more clinical samples to increase the credibility and clinical significance of our findings. Likewise, further studies are warranted to dissect the upstream regulatory factors and downstream ubiquitination targets of RNF2 and other epigenetic modifications involved in CHS development. Reportedly, proteolysis-targeting chimera (PROTAC), which is a technology targeting proteins by hijacking the ubiquitin-proteasome system, is in clinical trials as a cancer therapy [45]. Accordingly, PROTAC may be a useful tool for future the clinical treatment of CHS.

Supplementary Information

The online version contains supplementary material available at https://doi.org/10.1186/s40170-024-00359-x.

Supplementary Material 1

Supplementary Material 2

Supplementary Material 3

Acknowledgements

Not applicable.

Author contributions

YW, ZH are the guarantors of integrity of the entire study and contributed to the study concepts; PL contributed to the the data analysis, data acquisition; ZX, YW contributed to the study design, definition of intellectual content; MZ, ZH and ZWC contributed to the literature research, manuscript preparation; YLZ, JML contributed to the clinical studies, manuscript editing; PL, ZWC contributed to the statistical analysis, manuscript review; All authors read and approved the final manuscript.

Funding

This work was supported by Science and Education (2023) 4, Nanshan District Health Commission, Shenzhen (NS202304); Changsha Science and Technology Bureau Guiding Science and Technology Plan project (kzd22066).

Data availability

The data that support the findings of this study are available from the corresponding author upon reasonable request.

Declarations

Ethics approval and consent to participate

The patients were informed and signed an informed consent before specimen collection, and the study protocol and procedures were ratified by the Ethics Committee of The Fourth Hospital of Changsha, Changsha Hospital of Hunan Normal University (Approval number: 2023LL0901001). All procedures were strictly implemented according to the *Declaration of Helsinki*.

Consent for publication

All presentations of case reports have consent for publication.

Competing interests

The authors declare no competing interests.

Received: 9 May 2024 / Accepted: 16 October 2024
Published online: 25 October 2024

References

1. Mery B, Espenel S, Guy JB, Rancoule C, Vallard A, Aloy MT, Rodriguez-Lafrasse C, Magne N. Biological aspects of chondrosarcoma: leaps and hurdles. Crit Rev Oncol Hematol. 2018;126:32–6.
2. Heck RK Jr., Peabody TD, Simon MA. Staging of primary malignancies of bone. CA Cancer J Clin. 2006;56(6):366–75.
3. Herget GW, Strohm P, Rottenburger C, Kontny U, Krauss T, Bohm J, Sudkamp N, Uhl M. Insights into Enchondroma, Enchondromatosis and the risk of secondary Chondrosarcoma. Review of the literature with an emphasis on the clinical behaviour, radiology, malignant transformation and the follow up. Neoplasma. 2014;61(4):365–78.
4. Miwa S, Yamamoto N, Hayashi K, Takeuchi A, Igarashi K, Tsuchiya H. Therapeutic targets and emerging treatments in Advanced Chondrosarcoma. Int J Mol Sci 2022, 23(3).
5. Grimer RJ, Gosheger G, Taminiau A, Biau D, Matejovsky Z, Kollender Y, San-Julian M, Gherlinzoni F, Ferrari C. Dedifferentiated chondrosarcoma: prognostic factors and outcome from a European group. Eur J Cancer. 2007;43(14):2060–5.
6. Chow WA. Chondrosarcoma: biology, genetics, and epigenetics. *F1000Res* 2018, 7.
7. Gelderblom H, Hogendoorn PC, Dijkstra SD, van Rijswijk CS, Krol AD, Taminiau AH, Bovee JV. The clinical approach towards chondrosarcoma. Oncologist. 2008;13(3):320–9.
8. Jeong W, Kim HJ. Biomarkers of chondrosarcoma. J Clin Pathol. 2018;71(7):579–83.
9. Hershko A. Ubiquitin: roles in protein modification and breakdown. Cell. 1983;34(1):11–2.
10. Popovic D, Vucic D, Dikic I. Ubiquitination in disease pathogenesis and treatment. Nat Med. 2014;20(11):1242–53.
11. Mansour MA. Ubiquitination: friend and foe in cancer. Int J Biochem Cell Biol. 2018;101:80–93.
12. Pellegrino NE, Guven A, Gray K, Shah P, Kasture G, Nastke MD, Thakurta A, Gesta S, Vishnudas VK, Narain NR et al. The Next Frontier: Translational Development of Ubiquitination, SUMOylation, and NEDDylation in Cancer. Int J Mol Sci 2022, 23(7).
13. Zou T, Lin Z. The involvement of Ubiquitination Machinery in Cell Cycle Regulation and Cancer Progression. Int J Mol Sci 2021, 22(11).
14. Han S, Wang R, Zhang Y, Li X, Gan Y, Gao F, Rong P, Wang W, Li W. The role of ubiquitination and deubiquitination in tumor invasion and metastasis. Int J Biol Sci. 2022;18(6):2292–303.
15. Wu MH, Lee CY, Huang TJ, Huang KY, Tang CH, Liu SH, Kuo KL, Kuan FC, Lin WC, Shi CS. MLN4924, a protein neddylation inhibitor, suppresses the growth of human chondrosarcoma through inhibiting cell proliferation and inducing endoplasmic reticulum stress-related apoptosis. Int J Mol Sci 2018, 20(1).
16. Chen C, Zhou H, Zhang X, Liu Z, Ma X. Association of FBXW11 levels with tumor development and prognosis in chondrosarcoma. Cancer Biomark. 2022;35(4):429–37.
17. Yan Q, Chen BJ, Hu S, Qi SL, Li LY, Yang JF, Zhou H, Yang CC, Chen LJ, Du J. Emerging role of RNF2 in cancer: from bench to bedside. J Cell Physiol. 2021;236(8):5453–65.
18. Wang J, Ouyang X, Zhou Z, Mao S, Niu X, Li H, Xu W, Song Y, Cao J, Lai B. RNF2 promotes the progression of colon cancer by regulating ubiquitination and degradation of IRF4. Biochim Biophys Acta Mol Cell Res. 2022;1869(1):119162.
19. van Wijnen AJ, Bagheri L, Badreldin AA, Larson AN, Dudakovic A, Thaler R, Paradise CR, Wu Z. Biological functions of chromobox (CBX) proteins in stem cell self-renewal, lineage-commitment, cancer and development. Bone. 2021;143:115659.
20. Naqvi AAT, Rizvi SAM, Hassan MI. Pan-cancer analysis of Chromobox (CBX) genes for prognostic significance and cancer classification. Biochim Biophys Acta Mol Basis Dis. 2023;1869(1):166561.
21. Huang Z, Yan Y, Zhu Z, Liu J, He X, Dalangood S, Li M, Tan M, Cai J, Tang P, et al. CBX7 suppresses urinary bladder cancer progression via modulating AKR1B10-ERK signaling. Cell Death Dis. 2021;12(6):537.
22. Kim HY, Park JH, Won HY, Lee JY, Kong G. CBX7 inhibits breast tumorigenicity through DKK-1-mediated suppression of the Wnt/beta-catenin pathway. FASEB J. 2015;29(1):300–13.
23. Schmittgen TD, Livak KJ. Analyzing real-time PCR data by the comparative C(T) method. Nat Protoc. 2008;3(6):1101–8.
24. Chen J, Yu Y, Li H, Hu Q, Chen X, He Y, Xue C, Ren F, Ren Z, Li J, et al. Long non-coding RNA PVT1 promotes tumor progression by regulating the miR-143/HK2 axis in gallbladder cancer. Mol Cancer. 2019;18(1):33.
25. Sun X, Chen Y, Yu H, Machan JT, Alladin A, Ramirez J, Taliano R, Hart J, Chen Q, Terek RM. Anti-miRNA Oligonucleotide Therapy for Chondrosarcoma. Mol Cancer Ther. 2019;18(11):2021–9.
26. Cisowski J, Sayin VI, Liu M, Karlsson C, Bergo MO. Oncogene-induced senescence underlies the mutual exclusive nature of oncogenic KRAS and BRAF. Oncogene. 2016;35(10):1328–33.
27. Folkman J. Tumor angiogenesis: therapeutic implications. N Engl J Med. 1971;285(21):1182–6.
28. Lugano R, Ramachandran M, Dimberg A. Tumor angiogenesis: causes, consequences, challenges and opportunities. Cell Mol Life Sci. 2020;77(9):1745–70.
29. Gazendam A, Popovic S, Parasu N, Ghert M. Chondrosarcoma: a clinical review. J Clin Med 2023, 12(7).
30. Micaily I, Roche M, Ibrahim MY, Martinez-Outschoorn U, Mallick AB. Metabolic pathways and targets in Chondrosarcoma. Front Oncol. 2021;11:772263.
31. Marsh DJ, Dickson KA. Writing histone monoubiquitination in human malignancy-the role of RING finger E3 Ubiquitin Ligases. Genes (Basel) 2019, 10(1).
32. Sanchez-Molina S, Figuerola-Bou E, Blanco E, Sanchez-Jimenez M, Taboas P, Gomez S, Ballare C, Garcia-Dominguez DJ, Prada E, Hontecillas-Prieto L et al. RING1B recruits EWSR1-FLI1 and cooperates in the remodeling of chromatin necessary for Ewing sarcoma tumorigenesis. *Sci Adv* 2020, 6(43).
33. Wang Q, Wu Y, Lin M, Wang G, Liu J, Xie M, Zheng B, Shen C, Shen J. BMI1 promotes osteosarcoma proliferation and metastasis by repressing the transcription of SIK1. Cancer Cell Int. 2022;22(1):136.
34. Wen W, Peng C, Kim MO, Ho Jeong C, Zhu F, Yao K, Zykova T, Ma W, Carper A, Langfald A, et al. Knockdown of RNF2 induces apoptosis by regulating MDM2 and p53 stability. Oncogene. 2014;33(4):421–8.
35. Zhang J, Sun Z, Han Y, Yao R, Yue L, Xu Y, Zhang J. Rnf2 knockdown reduces cell viability and promotes cell cycle arrest in gastric cancer cells. Oncol Lett. 2017;13(5):3817–22.
36. Zheng N, Shabek N. Ubiquitin ligases: structure, function, and Regulation. Annu Rev Biochem. 2017;86:129–57.
37. Gong Y, Chen Y. UbE3-APA: a bioinformatic strategy to elucidate ubiquitin E3 ligase activities in quantitative proteomics study. Bioinformatics. 2022;38(8):2211–8.
38. Zhou J, Chen Z, Zou M, Wan R, Wu T, Luo Y, Wu G, Wang W, Liu T. Prognosis and Immune Infiltration of Chromobox Family genes in Sarcoma. Front Oncol. 2021;11:657595.
39. Forzati F, Federico A, Pallante P, Abbate A, Esposito F, Malapelle U, Sepe R, Palma G, Troncone G, Scarfo M, et al. CBX7 is a tumor suppressor in mice and humans. J Clin Invest. 2012;122(2):612–23.
40. Maimaitirexiati G, Tian P, Maimaiti H, Ding L, Ma C, Li Y, Wang J, Yan Q, Li R. Expression and correlation analysis of Skp2 and CBX7 in cervical cancer. J Clin Pathol. 2022;75(12):851–6.
41. Li R, Yan Q, Tian P, Wang Y, Wang J, Tao N, Ning L, Lin X, Ding L, Liu J, et al. CBX7 inhibits cell growth and motility and induces apoptosis in Cervical Cancer cells. Mol Ther Oncolytics. 2019;15:108–16.
42. Pallante P, Forzati F, Federico A, Arra C, Fusco A. Polycomb protein family member CBX7 plays a critical role in cancer progression. Am J Cancer Res. 2015;5(5):1594–601.
43. Huang J, Zhang W, Lin D, Lian L, Hong W, Xu Z. Chromobox Homologue 7 Acts as a Tumor Suppressor in Both Lung Adenocarcinoma and Lung Squamous Cell Carcinoma via Inhibiting ERK/MAPK Signaling Pathway. *Evid Based Complement Alternat Med* 2022, 2022:4952185.
44. Chen F, Hou W, Yu X, Wu J, Li Z, Xu J, Deng Z, Chen G, Liu B, Yin X, et al. CBX4 deletion promotes tumorigenesis under Kras(G12D) background by inducing genomic instability. Signal Transduct Target Ther. 2023;8(1):343.
45. Li J, Chen X, Lu A, Liang C. Targeted protein degradation in cancers: Orthodox PROTACs and beyond. Innov (Camb). 2023;4(3):100413.

Publisher's note